Double Fe-impurity charge state in the topological insulator Bi_2Se_3

V. S. Stolyarov,[1,2,3,4,5,6,a)] S. V. Remizov,[7,8] D. S. Shapiro,[7,8,2] S. Pons,[1] S. Vlaic,[1] H. Aubin,[1] D. S. Baranov,[2,3,9] Ch. Brun,[9] L. V. Yashina,[4] S. I. Bozhko,[3] T. Cren,[9] W. V. Pogosov,[2,7,10] and D. Roditchev[1,2,9]

[1]*Laboratoire de Physique et d'Etudes des Materiaux, ESPCI-Paris, CNRS and UPMC Univ Paris 6-UMR 8213, 10 rue Vauquelin, 75005 Paris, France*
[2]*Moscow Institute of Physics and Technology, 141700 Dolgoprudny, Russia*
[3]*Institute of Solid State Physics, Russian Academy of Sciences, 142432 Chernogolovka, Russia*
[4]*Moscow State University, 119992 Moscow, Russia*
[5]*National University of Science and Technology MISIS, 119049 Moscow, Russia*
[6]*Solid State Physics Department, KFU, 420008 Kazan, Russia*
[7]*Dukhov Research Institute of Automatics (VNIIA), 127055 Moscow, Russia*
[8]*Kotel'nikov Institute of Radio-engineering and Electronics, Russian Academy of Sciences, 125009 Moscow, Russia*
[9]*Institut des Nanosciences de Paris, Sorbonne Universites, UPMC Univ Paris 6 and CNRS-UMR 7588, F-75005 Paris, France*
[10]*Institute of Theoretical and Applied Electrodynamics, Russian Academy of Sciences, 125412 Moscow, Russia*

(Received 30 August 2017; accepted 1 December 2017; published online 18 December 2017)

The influence of individual impurities of Fe on the electronic properties of topological insulator Bi_2Se_3 is studied by Scanning Tunneling Microscopy. The microscope tip is used in order to remotely charge/discharge Fe impurities. The charging process is shown to depend on the impurity location in the crystallographic unit cell, on the presence of other Fe impurities in the close vicinity, and on the overall doping level of the crystal. We present a qualitative explanation of the observed phenomena in terms of tip-induced local band bending. Our observations evidence that the specific impurity neighborhood and the position of the Fermi energy with respect to both the Dirac point and bulk bands have to be taken into account when considering the electron scattering on the disorder in topological insulators. *Published by AIP Publishing.*
https://doi.org/10.1063/1.5002567

The uniqueness of the electronic properties of topological insulators (TIs) and specifically the topological protection of conduction electrons in these materials make them interesting for applications in quantum electronics.[1–5] The understanding of the impurity scattering effects on the properties of TIs is therefore of primary importance.[6–10] In this context, the role of magnetic impurities is still unclear as their presence may lead to rather complicated phenomena.[11] For instance, magnetic impurities in TIs can support long-range magnetic order,[6,12,13] open an energy gap at the Dirac point, and even result in the formation of a quantum anomalous Hall state.[14] The possibility to produce a long-range ordering of impurity spins could be of great interest for realization of novel electronic states, quantum computing, and spintronics.[15]

With the charge screening being rather poor in Dirac materials, individual atomic impurities are likely to be charged. This charging could have a dramatic impact on the efficiency of novel field-effect nano-devices[16] based on topological insulators. Charged individual Fe-impurities embedded in Bi_2Se_3 have already been reported in previous works[15,17,18] and produce ring-shaped spectral features in conductance images of scanning tunneling microscopy (STM) experiments. Also, the observation of impurity charging is not exclusive to TIs: ionization rings were observed near defects in several materials such as semiconductors,[19–24] graphene,[25] and semiconductor surfaces with deposited Co-islands.[26] In our work, we show that the position of the Fermi energy with respect to the Dirac point and the bulk bands[27] plays a crucial role in the charge screening and scattering in TIs. We also evidence the strong influence of neighboring impurities in the charging of an individual iron atom.

Our experiments were done by means of 3 complementary experimental techniques. Scanning Tunneling Microscopy/Spectroscopy (STM/STS), Atomic Force Microscopy (AFM), and Angle Resolved Photoemission Spectroscopy (ARPES) were used for the study of Bi_2Se_3 single crystals in which 0.2% of Fe-impurities were incorporated. The studied samples were cleaved *in situ* under ultra-high vacuum. This procedure enables the production of atomic clean surfaces with Fe impurities protected from oxidation imbedded in the first crystallographic planes.

The implanted Fe atoms produce at least three typical kinds of punctual defects shown in Fig. 1, each having a characteristic topographic fingerprint and a specific spectral signature in STM images. Fe atoms may either occupy interstitial sites or substitute isovalent two distinct Bi sites at the subsurface.[15] The surface plane of Bi_2Se_3 is composed of Se atoms so the location of Fe impurities in the lower atomic planes can be evidenced by simultaneous AFM-STM imaging: AFM imaging [see Figs. 2(a) and 2(b)] does not show any chemical contrast in the Se atomic lattice of the surface plane where the tunneling current reveals the presence of triangular electronic patterns due to the scattering of the electronic states on the buried impurity. In agreement with previous works, we can identify these impurities in Fig. 1(a). Fe substitution at Bi sites

a)Electronic mail: vasiliy@travel.ru

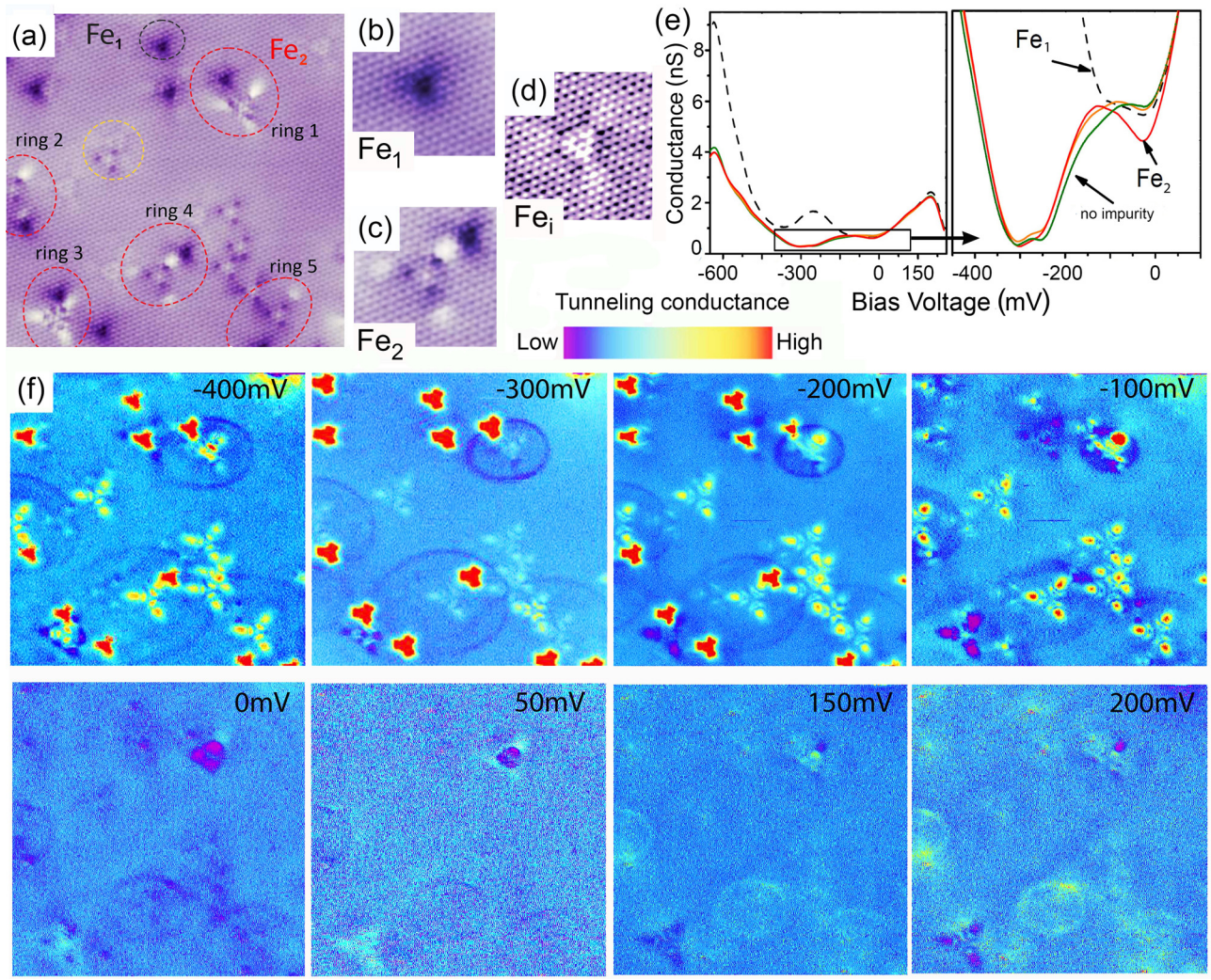

FIG. 1. (a) STM topography image of $Fe_{0.2\%}$ Bi_2Se_3. $V_{sample} = 103\,mV$ and $I = 177\,pA$. $26 \times 26\,nm^2$. (b)–(d) zoom on Fe_1, Fe_2, and Fe_i, respectively. $6 \times 6\,nm^2$. (e) Spectral signatures of the defects recorded by STS on Fe_1 and Fe_2 impurities and compared to the average spectrum. (f) Conductance images recorded at the same location than the topography image (a). Stabilization parameters: $V_{sample} = 102.5\,mV$ and $I = 180\,pA$. All STM/STS data were obtained at temperature $T = 1.5\,K$.

in the second atomic layer from the surface is most often observed,[15] Fig. 1(b); these defects are denoted Fe_1 in the following. Other characteristic defects –Fe_2– are associated with Fe substitution at Bi sites in the fourth atomic layer from the surface, Fig. 1(c) [for clearness, see Fig. 2(c)]. In addition to these defects, a low concentration of Fe atoms occupying interstitial sites –Fe_i– is also observed, Fig. 1(d).

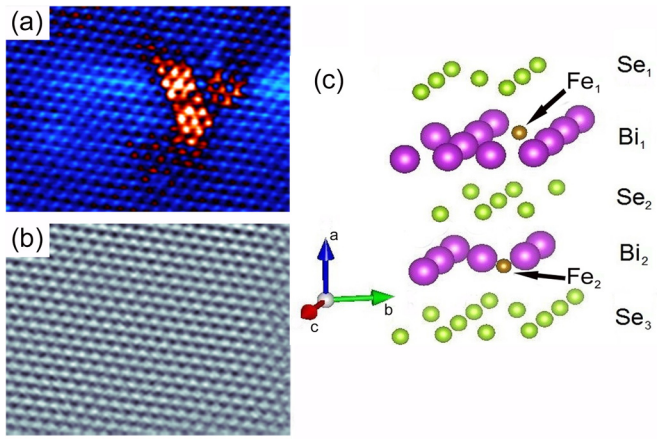

FIG. 2. AFM-STM image of a buried impurity and crystal structure of Bi_2Se_3. (a) Current image; (b) AFM simultaneous image. The feedback was made in te AFM mode by keeping a constant frequency shift of 1 Hz. (c) Two Fe substitutions for Bi sites are labeled Fe_1 and Fe_2, respectively.

A selection of $dI/dV(V)$ conductance images recorded by scanning tunneling spectroscopy and measured above and below the Fermi level E_F^s is presented in Fig. 1(e). All these images were recorded in the area presented in topographic image in Fig. 1(a). In our experiments, Fe_1 defects exhibit a specific spectral signature at $-300\,mV$ presented in Fig. 1(e), giving rise to a strongly contrasted triangular shape in conductance images at negative voltages in Fig. 1(f). Fe_2 sites do not show any sharp signatures in the conductance spectra, Fig. 1(e), but they also exhibit regular patterns with triangular symmetry in the conductance images at negative voltages. Finally, Fe_i sites only weakly perturb the electronic properties.

Circular patterns due to charging of Fe impurities are also visible in conductance images. The rings are seen to appear only around some specific defects and some defects are not related to charging rings. The ring contrast is dark for bias voltages ranging from $-500\,mV$ to $+100\,mV$ applied to the sample with respect to the tip. On the contrary, from $+100\,mV$

to +250 mV, the rings appear brighter. It has been shown in prior works that the observed rings can be unambiguously associated with the charging/discharging of specific impurities, triggered by the STM tip. With the density of the conduction states being low, the presence of a metallic tip at biased voltage near the surface results in a local band bending in the sample below the tip. For a better understanding of this phenomenon, one can evoke a certain analogy between tip-induced band bending and the working principle of a MOS-FET: the biased tip and the vacuum barrier of the STM junction play the same respective roles as the metallic gate and the oxide layer in the FET. The band bending depends on the bias voltage of the tip with respect to the sample and also on the position of the tip. At certain defect-tip separation, the tip-induced band bending at the position of the defect can become significant enough to trigger its ionization. The Coulomb field of the ionized impurity produces an additional band shifting around a dopant. Consequently, the electron tunneling conditions through the STM junction are modified, resulting in circular features around dopants in tunneling conductance images. The imperfect circular symmetry of spectral features is mainly imposed by the symmetry of the electrostatic stray field of the imperfect conical tip.

Fe dopants are expected to exhibit two charge states in Bi_2Se_3: Fe^{3+} and Fe^{2+}. The Fe^{2+} state is more energetically favorable for Fermi level E_F^s located closer to the conduction band minimum, while Fe^{3+} dominates[28] for lower E_F^s. In the first case, the ionization of Fe^{2+} into Fe^{3+} should occur under the upward band bending (sample voltages exceed flat-band voltage V_{FB}), while the ionization ring radius grows with the increase in the sample voltage. In the second case, the ionization of Fe^{3+} into Fe^{2+} is possible under the downward band bending (sample voltage is lower than the flat-band voltage V_{FB}), while the ionization ring radius must grow with the decrease in the sample voltage. The latter scenario is consistent with our observations of the dependence of ionization ring radii on the sample voltage (Fig. 3) and with previously reported results[15] where Fe dopants were considered in the 3+ state in the absence of STM tip. Thus, we conclude that the ionization rings observed in our experiments are associated with tip-induced switching of the dopant state from Fe^{3+} into Fe^{2+}. Details regarding mechanisms of Fe impurity ionization under tip-induced band bending can be found in the supplementary material.

Although the basic physics behind our observation seems established,[15,17,18,28] we discovered two remarkable features which were not evidenced in prior works: (i) not all the defects exhibit charging rings in their vicinity and (ii) the charging rings are revealed at both positive and negative voltages in our study and they manifest a puzzling contrast reversal. In order to understand these new features, we first analyze the local environment of the charging rings. A closer inspection reveals that the rings are observed only around a very peculiar type of defects which have a composite nature. Individual Fe atoms do not provoke ionization rings in our sample. It is seen from STS images that the charging rings are always enclosing two impurities one being of Fe_2 nature and the other one of Fe_1 kind. These defects are separated by a few interatomic distances and form a doublet. The origin of this phenomenon seems to come from the position of E_F^s.

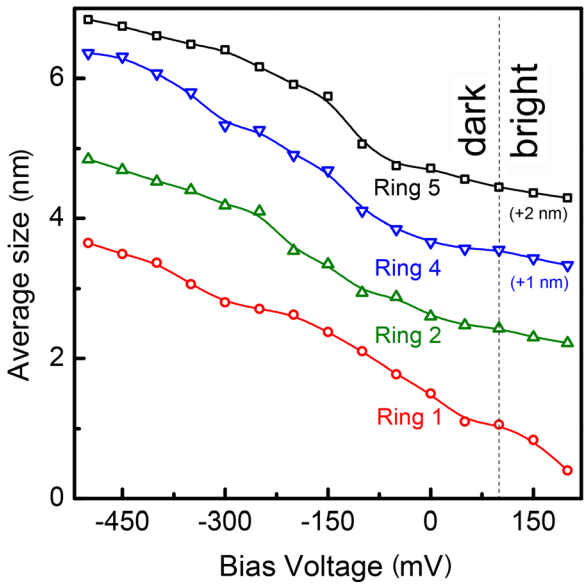

FIG. 3. Evolution of the radius of ionization rings as a function of sample bias: $\sqrt{ab}/\pi$, where a and b are semi-axes of the elliptic rings. The spectral contrast switches from dark (at negative sample biases) to bright at approximately +100 mV. For clarity, +1 and +2 indicate that the average size is increased by +1 and +2 nm.

From our ARPES experiments (Fig. 4), we have established that E_F^s of our heavily Fe doped samples ($Fe_{0.2\%}Bi_2Se_3$) is located in the bulk conduction band, i.e., at higher energy than that of the previously studied samples. The position of E_F^s can be also lifted by native defects.[29] A high E_F^s should yield single defects to be in the Fe^{2+} state.[28] Thus, our Fe doped samples have to intrinsically exhibit Fe^{2+} sites prior to any STM experiment. Therefore, once the tip is brought towards the sample surface during STM experiments, a downward tip-induced band bending will not result in any ionization of a single defect irrespective of its nature (Fe_1, Fe_2, or Fe_i). On the contrary, upward band bending would result in an ionization of the defects. We believe that such an ionization from Fe^{2+} into Fe^{3+} was not observed in our experiments since the highest sample voltage applied, +250 mV, was too low, while V_{FB} in our experiment could be positive. Although an extraction of a precise value of V_{FB} is known to be a

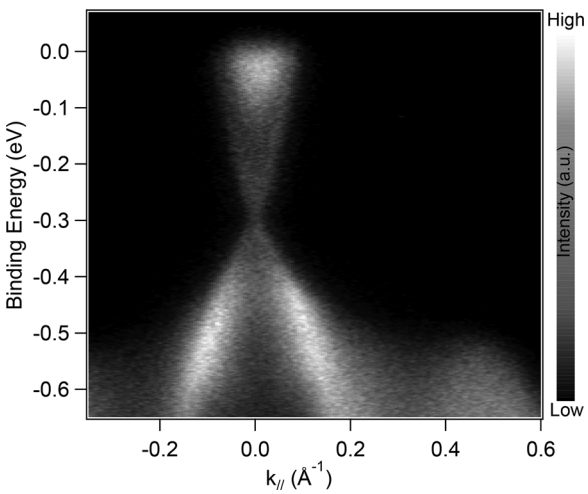

FIG. 4. ARPES intensity image of $Fe_{0.2}Bi_2Se_3$ taken at T = 10 K along the $\bar{\Gamma} - \bar{\mathbf{M}}$ direction with photons of 21.2 eV.

complicated task, simple considerations show that its sign in our experiments might be highly sensitive to the shape and sizes of our tip, since the work function for a platinum-iridium alloy of the tip is nearly the same as the electron affinity of Bi_2Se_3 equal to 5.3 eV.[30] Under positive V_{FB}, bands are bend downward by the tip already at zero voltage. This could be a reason why the ionization from Fe^{2+} into Fe^{3+} was not observed.

However, our experimental data evidence that the presence of the Fe_1 defect in the surrounding of the Fe_2 defect [see Fig. 1(f)] gives rise to a different situation leading to the tip-induced ionization of the Fe_2 defect. The ionization ring radius grows with the decrease in sample voltage, which implies that the Fe_2 defect in the doublet is intrinsically in the Fe^{3+} state. The microscopic mechanism for such an influence of the Fe_1 defect on the charge state of the Fe_2 defect is not so clear and deserves a separate study, but it might be related to the local shift of the band structure around the Fe_1 impurity. This possible mechanism is discussed further in the supplementary material.

Another argument in support of our picture comes from the analysis of the contrast of the ring as a function of bias voltage in conductance images, e.g., Figs. 1(c) and 1(f). Most of the rings appear bright at positive sample voltages and dark at negative sample voltages. A similar behavior has been reported in paper[26] (see also paper[31]) where Co islands on InAs surfaces have been studied. In Co/InAs, E_F^s is also above the conduction band minimum, in analogy with our samples, so it is natural to assume that this feature plays an important role in changing ring contrast. Indeed, ionization from Fe^{3+} into Fe^{2+} increases the number of filled states in the valence band but decreases their number in the conduction band, which results in the interplay between the two opposite contributions to the conductance. Details regarding this competition, as well as an analysis of a connection between ring sizes and the STM tip shape, can be found in the supplementary material.

In summary, we characterized and locally manipulated the electronic states of Fe dopants in Bi_2Se_3 crystals. In our experiments, because of the high E_F^s in our sample (due to heavy doping and native defects), the presence of Fe_1 impurities has been shown to allow for the charging process under the scanning tunneling tip. Fe_1 defects modify the transition threshold from one charge state to another of Fe_2 impurities in the neighborhood, possibly by locally doping the system with holes. Thus, the composite structure of the defect is essential for the charge manipulation. Our observations evidence that the specific impurity neighborhood and the position of the Fermi energy have to be taken into account when considering the electron scattering on the disorder in topological insulators. Our work opens an interesting opportunity of engineering the charge (and magnetic) state of dopants in topological insulators by adding specific impurities in their surrounding favoring or blocking their ionization.

See supplementary material for the description of details on ionization mechanisms and for the analysis of a relation between the STM tip shape and ionization ring characteristics.

The authors acknowledge useful discussions with D. Muzychenko, A. A. Ezhov, and S. V. Zaitsev-Zotov. The work of V.S., D.S., D.B., and W.P. was supported by Grants of Ministry of Education and Science of the Russian Federation in the frame work of the Federal Target Program "Research and development in priority areas of science and technology complex of Russia for 2014–2020," Grant No. 14Y.26.31.0007. The ARPES studies were supported by RFBR 16-02-00727 and 17-52-50080. French authors: D.R., S.P., S.V., H.A., and T.C. acknowledge ANR (SUPERSTRIPES, MISTRAL) and D.R. and S.P. acknowledge C'NANO Ile-de-France, DIM NanoK, for their support of the Nanospecs project. V.S. gratefully acknowledges the financial support of the Ministry of Education and Science of the Russian Federation in the framework of Increase Competitiveness Program of NUST ≪MISiS≫ (No. K3-2017-042), implemented by a governmental decree dated 16th of March 2013, N 211. We thank for partial support by the Program of Competitive Growth of Kazan Federal University.

[1]M. Z. Hasan and C. L. Kane, Rev. Mod. Phys. **82**, 3045 (2010).
[2]X.-L. Qi and S.-C. Zhang, Rev. Mod. Phys. **83**, 1057 (2011).
[3]L. Fu, C. L. Kane, and E. J. Mele, Phys. Rev. Lett. **98**, 106803 (2007).
[4]J. E. Moore and L. Balents, Phys. Rev. B **75**, 121306(R) (2007).
[5]D. Hsieh, Y. Xia, D. Qian, L. Wray, J. H. Dil, F. Meier, J. Osterwalder, L. Patthey, J. G. Checkelsky, N. P. Ong, A. V. Fedorov, H. Lin, A. Bansil, D. Grauer, Y. S. Hor, R. J. Cava, and M. Z. Hasan, Nature **460**, 1101 (2009).
[6]Y. L. Chen, J.-H. Chu, J. G. Analytis, Z. K. Liu, K. Igarashi, H.-H. Kuo, X. L. Qi, S. K. Mo, R. G. Moore, D. H. Lu, M. Hashimoto, T. Sasagawa, S. C. Zhang, I. R. Fisher, Z. Hussain, and Z. X. Shen, Science **329**, 659 (2010).
[7]Y. Cui, N. Nilius, H.-J. Freund, S. Prada, L. Giordano, and G. Pacchioni, Phys. Rev. B **88**, 205421 (2013).
[8]A. Polyakov, H. L. Meyerheim, E. D. Crozier, R. A. Gordon, K. Mohseni, S. Roy, A. Ernst, M. G. Vergniory, X. Zubizarreta, M. M. Otrokov, E. V. Chulkov, and J. Kirschner, Phys. Rev. B **92**, 045423 (2015).
[9]M. M. Yee, Z.-H. Zhu, A. Soumyanarayanan, Y. He, C.-L. Song, E. Pomjakushina, Z. Salman, A. Kanigel, K. Segawa, Y. Ando, and J. E. Hokman, Phys. Rev. B **91**, 161306 (2015).
[10]T. Eelbo, M. Wasniowska, M. Sikora, M. Dobrzanski, A. Kozlowski, A. Pulkin, G. Autes, I. Miotkowski, O. V. Yazyev, and R. Wiesendanger, Phys. Rev. B **89**, 104424 (2014).
[11]S.-Y. Xu, M. Neupane, C. Liu, D. Zhang, A. Richardella, L. A. Wray, N. Alidoust, M. Leandersson, T. Balasubramanian, J. Sanchez-Barriga, O. Rader, G. Landolt, B. Slomski, J. H. Dil, J. Osterwalder, T.-R. Chang, H.-T. Jeng, H. Lin, A. Bansil, N. Samarth, and M. Z. Hasan, Nat. Phys. **8**, 616 (2012).
[12]Y. S. Hor, P. Roushan, H. Beidenkopf, J. Seo, D. Qu, J. G. Checkelsky, L. A. Wray, D. Hsieh, Y. Xia, S.-Y. Xu, D. Qian, M. Z. Hasan, N. P. Ong, A. Yazdani, and R. J. Cava, Phys. Rev. B **81**, 195203 (2010).
[13]L. A. Wray, S. Y. Xu, Y. Xia, D. Hsieh, A. V. Fedorov, Y. San Hor, R. J. Cava, A. Bansil, H. Lin, and M. Z. Hasan, Nat. Phys. **7**, 32 (2011).
[14]R. Yu, W. Zhang, H. J. Zhang, S. C. Zhang, X. Dai, and Z. Fang, Science **329**, 61 (2010).
[15]C.-L. Song, Y.-P. Jiang, Y.-L. Wang, Z. Li, L. Wang, K. He, X. Chen, X.-C. Ma, and Q.-K. Xue, Phys. Rev. B **86**, 045441 (2012).
[16]F. Xiu, L. He, Y. Wang, L. Cheng, L. T. Chang, M. Lang, G. Huang, X. F. Kou, Y. Zhou, X. W. Jiang, Z. G. Chen, J. Zou, A. Shailos, and K. L. Wang, Nat. Nanotechnol. **6**, 216 (2011).
[17]D. West, Y. Y. Sun, S. B. Zhang, T. Zhang, X. C. Ma, P. Cheng, Y. Y. Zhang, X. Chen, J. F. Jia, and Q. K. Xue, Phys. Rev. B **85**, 081305 (2012).
[18]T. Schlenk, M. Bianchi, M. Koleini, A. Eich, O. Pietzsch, T. O. Wehling, T. Frauenheim, A. Balatsky, J.-L. Mi, B. B. Iversen, J. Wiebe, A. A. Khajetoorians, P. Hofmann, and R. Wiesendanger, Phys. Rev. Lett. **110**, 126804 (2013).
[19]D. H. Lee and J. A. Gupta, Nano Lett. **11**, 2004 (2011).
[20]K. Teichmann, M. Wenderoth, S. Loth, R. G. Ulbrich, J. K. Garleff, A. P. Wijnheijmer, and P. M. Koenraad, Phys. Rev. Lett. **101**, 076103 (2008).

[21]A. P. Wijnheijmer, J. K. Garleff, K. Teichmann, M. Wenderoth, S. Loth, R. G. Ulbrich, P. A. Maksym, M. Roy, and P. M. Koenraad, Phys. Rev. Lett. **102**, 166101 (2009).
[22]F. Marczinowski, J. Wiebe, J.-M. Tang, M. E. Flatté, F. Meier, M. Morgenstern, and R. Wiesendanger, Phys. Rev. Lett. **99**, 157202 (2007).
[23]H. Zheng, A. Weismann, and R. Berndt, Phys. Rev. Lett. **110**, 226101 (2013).
[24]H. Zheng, J. Zhang, and R. Berndt, Sci. Rep. **7**, 10764 (2017).
[25]V. W. Brar, R. Decker, H.-M. Solowan, Y. Wang, L. Maserati, K. T. Chan, H. Lee, C. O. Girit, A. Zettl, S. G. Louie, M. L. Cohen, and M. F. Crommie, Nat. Phys. **7**, 43 (2011).
[26]D. A. Muzychenko, K. Schouteden, S. V. Savinov, N. S. Maslova, V. I. Panov, and C. Van Haesendonck, J. Nanosci. Nanotechnol. **9**, 4700 (2009).
[27]A. A. Kapustin, V. S. Stolyarov, S. I. Bozhko, D. N. Borisenko, and N. N. Kolesnikov, J. Exp. Theor. Phys. **121**(2), 279 (2015).
[28]J.-M. Zhang, W. Ming, Z. Huang, G.-B. Liu, X. Kou, Y. Fan, K. L. Wang, and Y. Yao, Phys. Rev. B **88**, 235131 (2013).
[29]J. Suh, D. Fu, X. Liu, J. K. Furdyna, K. M. Yu, W. Walukiewicz, and J. Wu, Phys. Rev. B **89**, 115307 (2014).
[30]C. D. Spataru and F. Léonard, Phys. Rev. B **90**, 085115 (2014).
[31]J. W. G. Wildöer, A. J. A. van Roij, C. J. P. M. Harmans, and H. van Kempen, Phys. Rev. B **53**, 10695 (1996).